# Stratigraphy, structure and geochemistry of Archaean supracrustal rocks from Oqaatsut and Naajaat Qaqqaat, north-east Disko Bugt, West Greenland

*Henrik Rasmussen and Lars Frimodt Pedersen*

Two Archaean supracrustal sequences in the area north-east of Disko Bugt, *c.* 1950 and *c.* 800 m in thickness, are dominated by pelitic and semipelitic mica schists, interlayered with basic metavolcanic rocks. A polymict conglomerate occurs locally at the base of one of the sequences.

One of the supracrustal sequences has undergone four phases of deformation; the other three phases. In both sequences an early phase, now represented by isoclinal folds, was followed by north-west-directed thrusting. A penetrative deformation represented by upright to steeply inclined folds is only recognised in one of the sequences. Steep, brittle N–S and NW–SE striking faults transect all rock units including late stage dolerites and lamprophyres.

Investigation of major- and trace-element geochemistry based on discrimination diagrams for tectonic setting suggests that both metasediments and metavolcanic rocks were deposited in an environment similar to a modern back-arc setting.

H.R.* & L.F.P.‡, *Geological Institute, University of Copenhagen, Øster Voldgade 10, DK-1350 Copenhagen K, Denmark.* *Present address: *Mærsk Olie og Gas AS, Esplanaden 50, DK-1263 Copenhagen K, Denmark.* E-mail: *h_rasmussen@vip.cybercity.dk.* ‡Present address: *Falkenberg A/S, Højbrogade 12–14, DK-4800 Nykøbing F, Denmark.*

Keywords: Archaean, Disko Bugt, geochemistry, supracrustal rocks, West Greenland

The Precambrian terrain north-east of Disko Bugt consists of four main rock units: Archaean grey gneisses, Archaean supracrustal rocks, the 2800 Ma Atâ tonalite that intrudes supracrustal rocks and gneisses, and the early Proterozoic Anap nunâ Group (Garde & Steenfelt 1999, this volume).

Archaean supracrustal rocks are dominated by basic metavolcanic rocks and pelitic to semipelitic metasediments, which have been metamorphosed under greenschist to middle amphibolite facies conditions. The rocks are strongly deformed and folded into both tight and open structures as a result of several phases of Archaean and Proterozoic deformation.

This paper deals with the supracrustal rocks of Oqaatsut and Naajaat Qaqqaat, located south and north of the fjord Torsukattak, respectively (Fig. 1). These rocks were briefly investigated during the early regional mapping of the Disko Bugt area (Escher & Burri 1967), but detailed structural and stratigraphical investigations have not been carried out previously, and no geochemical data were available.

## Stratigraphy

### Oqaatsut

The supracrustal sequence on Oqaatsut is bounded to the west and east by granitoid rocks (Fig. 1). The succession has a general N–S trend and dips moderately to the east. It can be divided into three main units: a lower and an upper amphibolitic greenstone unit, with a metasedimentary unit in between (Fig. 2).

The metasedimentary unit has at present a maximum thickness of *c.* 1150 m in the centre of the island and a minimum thickness of about 850 m in the south. It is dominated by light to dark grey, fine-grained quartzofeldspatic metapelitic schists, often rich in biotite.

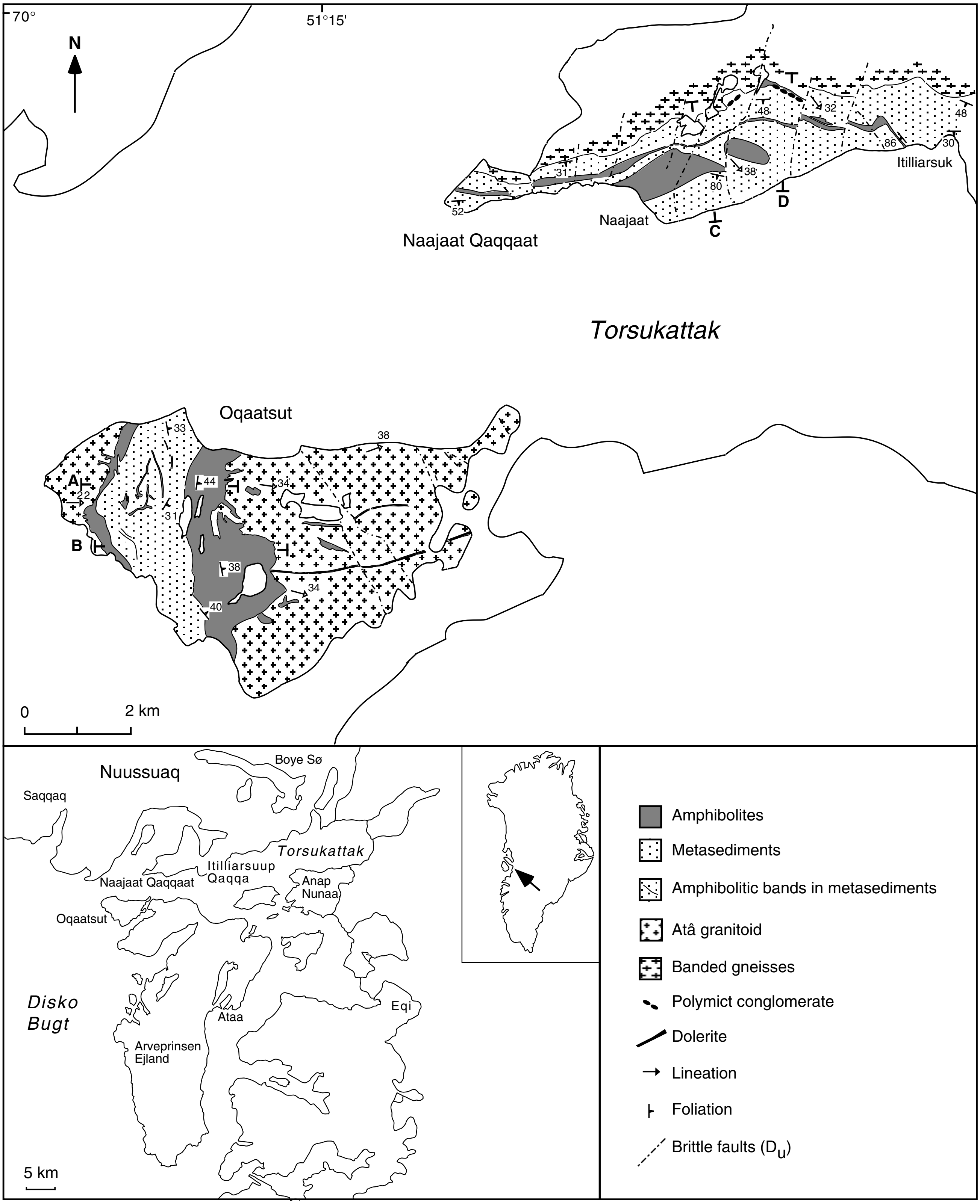

Fig. 1. Geological sketch map of Oqaatsut and Naajaat Qaqqaat, north-east Disko Bugt, West Greenland with location of the profiles A and B (Fig. 2), and C and D (Fig. 3).

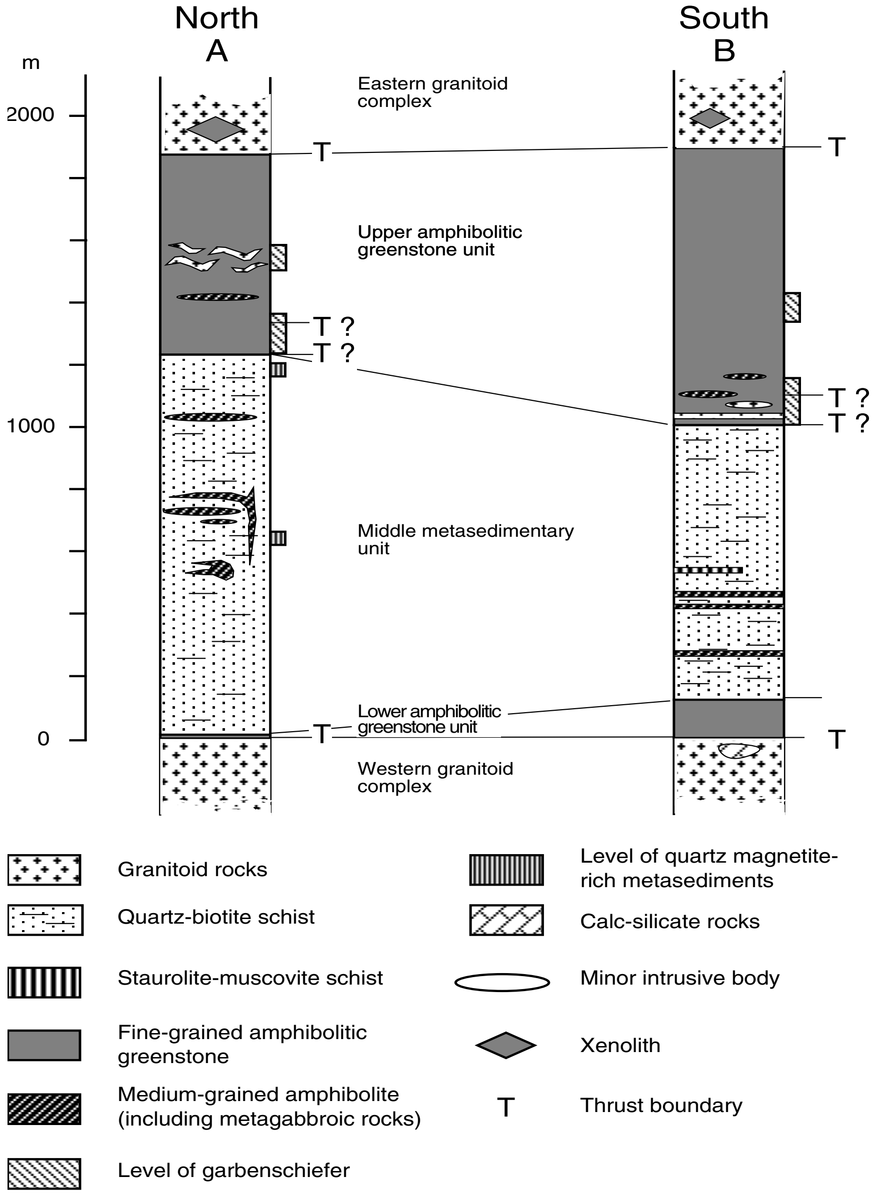

Fig. 2. Schematic stratigraphy of supracrustal rocks on Oqaatsut. For location of profiles A and B see Fig. 1.

Amphibole is sometimes present and pale blue kyanite was observed at a few localities, sometimes associated with garnet and staurolite. Porphyroblastic garnet is common throughout the entire unit. Minor amphibolitic layers and lenses are common, especially near the contact to the major greenstone units. Amphibolites found within the metasediments are mostly fine grained and occur both as foliation-parallel, sill-like layers and as cross-cutting dykes. The metasediments contain a few, 1–5 m thick, horizons of fine-grained staurolite-muscovite schist with staurolite porphyroblasts (1–3 mm), as well as 1–3 m thick horizons of fuchsite-bearing quartz-muscovite schist. Quartz-magnetite rich rocks were found at two localities as 1–2 m thick layers. They consist of alternating quartz and magnetite laminae a few millimetres to about 1–2 cm wide.

The tectonostratigraphically lower, western amphibolitic greenstone unit is 10–125 m thick. To the west it is disrupted by light grey, medium-grained granioid

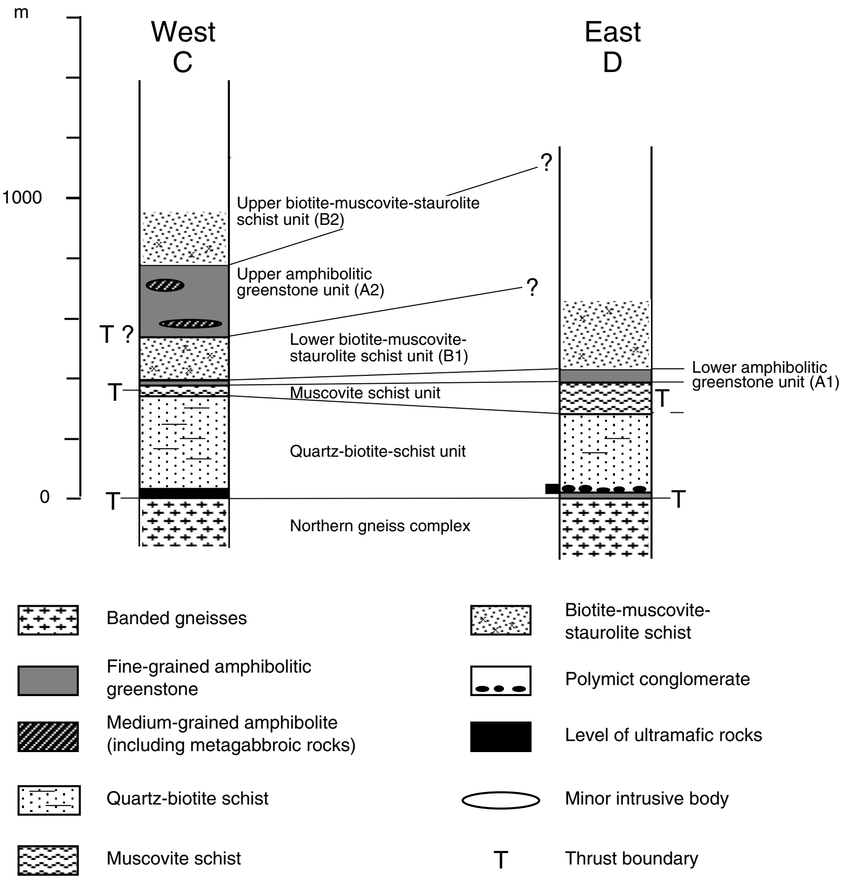

Fig. 3. Schematic stratigraphy of supracrustal rocks on Naajaat Qaqqaat. For location of profile C and D see Fig. 1.

rocks (Fig. 1), and to the east there is a gradual transition to the overlying metasedimentary unit. This lower unit mainly consists of fine-grained amphibolite with a few subordinate bodies of metagabbro. Garnet is found locally. Disseminated sulphides locally give rise to rusty weathering and local malachite staining on joint surfaces. Relationships between the western granitoid complex and the lower amphibolitic unit are not clear because of later shearing and folding at the boundary. The granitoids, however, are believed to be intrusive into the supracrustal rocks.

The upper amphibolitic greenstone unit (Fig. 2) forms a *c.* 900 m thick succession in the central part of the island. It thins both to the south and to the north, where it is *c.* 600 m thick. The amphibolites are mostly fine grained with local layers of garbenschiefer, but minor bodies and lenses of metagabbroic rocks with recognisable igneous textures are also present.

To the east the supracrustal sequence is overlain by granitoid rocks belonging to the 2800 Ma Atâ tonalite (Kalsbeek & Skjernaa 1999, this volume). Granitoid dykes are found in the upper amphibolitic greenstone unit, and xenoliths of amphibolite, up to *c.* 100 m in size, are observed within the granitoids, which clearly suggest they were intruded into the supracrustal sequence. Shear and thrust movements between the two units have resulted in the formation of a mylonitic border zone, within which both units have been strongly deformed.

Lamprophyres (*c.* 1750 Ma; Larsen & Rex 1992; Rasmussen & Holm 1999, this volume) are locally present in up to 1 m thick E–W-trending dykes within the northern and central parts of the eastern granitoids. They are fine grained with a brown to greenish appearance and sometimes show signs of strong internal shearing and deformation; they have not been identified within the supracrustal rocks. Subvertical E–W-trending dolerite dykes, 1 and 4 m thick, also occur in the granitoid rocks. Also these dykes could not be traced into the underlying supracrustal sequences.

## *Naajaat Qaqqaat*

The supracrustal sequence on Naajaat Qaqqaat is dominated by staurolite, muscovite and biotite-rich schists alternating with amphibolitic greenstone units (Fig. 3). It trends E–W with moderate dips towards S and SE,

Fig. 4. Folded conglomerate with drag fold near the base of the supracrustal succession at Naajaat Qaqqaat. The drag fold ($D_2$) in the conglomerate horizon is viewed in a south-easterly direction. The *Z* folds plunge moderately to the SE, subparallel with a mineral liniation.

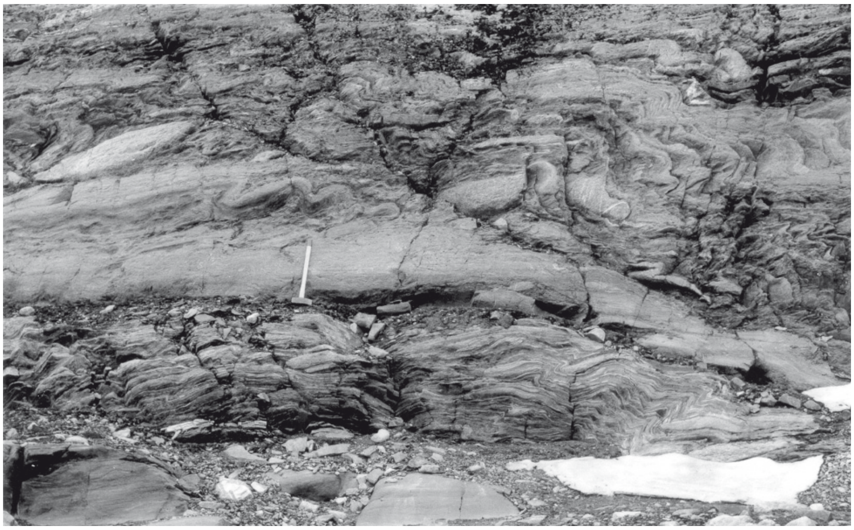

and rests on a strongly sheared and banded gneiss complex to the north. The contact with the gneisses is strongly sheared; nevertheless the gneiss complex is believed to form the basement of the supracrustal rocks.

The lowermost quartz-biotite schist unit on Naajaat Qaqqaat is between 150 and 350 m thick (Fig. 3). At Itilliarsuk in the easternmost part of the area, however, it reaches a tectonostratigraphical thickness of over 600 m. The dominant rock type is a light-grey schist, rich in quartz, feldspar and biotite. It is sometimes banded at a scale of 1 cm or less. Some horizons are garnetiferous, and hornblende and muscovite are found locally. At a few localities biotite-kyanite-staurolite-rich schists occur.

In the central part of Naajaat Qaqqaat, the base of the quartz-biotite schist unit is marked by a polymict conglomerate (Fig. 4), two exposures of which can be followed 200 m and 500 m along strike. The conglomerate is matrix supported and clasts consist mainly of amphibolite and foliated tonalite. The clasts, which are strongly sheared and folded, range in size from pebbles to cobbles, with a few reaching the size of boulders. A similar exposure of a polymict conglomerate has been reported from Itilliarsuup Qaqqaa (Garde & Steenfelt 1999, this volume). The basal conglomerate and the overlying metasediments indicate a transition from a shallow water environment, adjacent to an exposed area of older crust, towards a deeper water, oceanic environment.

The overlying biotite-muscovite-staurolite schists can be divided into a lower and upper unit (B1 and B2, Fig. 3). The lower unit extends along strike from Naajaat to Itilliarsuk. In this part of Naajaat Qaqqaat it varies in thickness from less than 100 m up to 350–400 m in the east. West of Naajaat it is only exposed in a few outcrops along the coast, and the thickness does not exceed 50 m. The upper unit (B2) has only been found just east of Naajaat along steep coastal cliffs. Because of poor accessibility its thickness is not known, but has been estimated to be at least 220 m. The rocks from the lower and upper units are texturally and mineralogically very similar, and occur in the field as brownish-red, medium- to coarse-grained mica-rich schists. Both biotite and muscovite are present in a matrix dominated by quartz and plagioclase. Garnet, often together with staurolite, is also present. Locally the schists contain kyanite, especially in the lower unit, often together with quartz lenses and veins.

The muscovite schist unit (Fig. 3) is an important marker and can be followed along strike from east to west across the entire area. In the western part this unit is thin, rarely exceeding 3–4 m. In the central part of the area it has a thickness of 50 m and just west of Itilliarsuk it reaches 100 m. It has a well-developed schistosity; in some exposures it is strongly sheared and transformed into a fine-grained banded mylonite. The muscovite schist consists predominantly of fine-grained quartz, feldspar and muscovite and locally contains minor pyrite, garnet and biotite.

Two units of amphibolitic greenstone are present at Naajaat Qaqqaat (Fig. 3, A1 and A2). The lower unit (A1) is continuous; it is approximately 100 m thick in the central eastern part of Naajaat Qaqqaat, but its thickness varies considerably, and at many places it does not exceed 10–20 m. Fine-grained amphibolite dominates this unit. It is foliated and may contain very thin

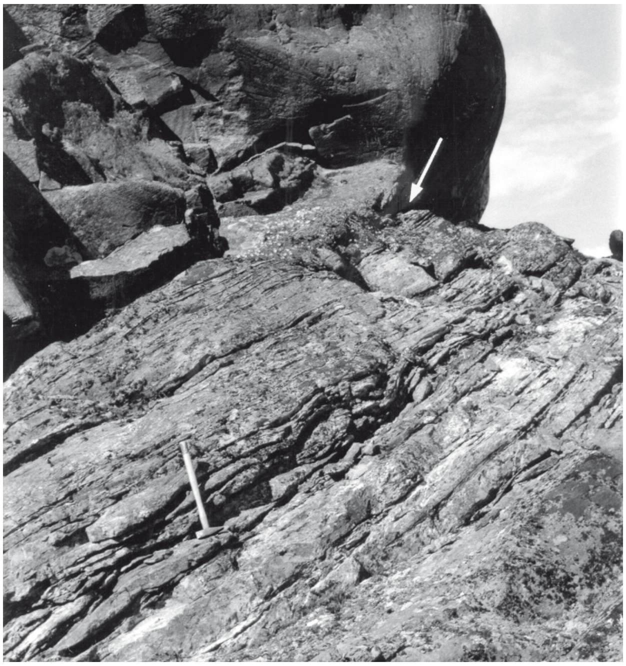

Fig. 5. Moderately SE-dipping sheared contact between the orthogneiss basement and supracrustal (ultramafic) rocks. The sharp contact is one metre above the hammer. Viewed towards west.

layers (up to 5 mm) of felsic material. In a few places more coarse-grained amphibolitic and metagabbroic layers were found. The upper amphibolitic unit is at least 250 m thick in central Naajaat Qaqqaat (Fig. 3), but further west it is only exposed in the coastal areas, where it is only 10–20 m thick. Like the lower greenstone unit, the upper unit is dominated by fine-grained, homogeneous to faintly laminated amphibolites interbedded with thin felsic horizons. Enclaves of medium-grained metagabbroic amphibolite are much more frequent than in the lower unit. Also lenses of hornblende-rich often garnetiferous amphibolite were found. Large (1–2 cm) garnet crystals in these amphibolites are partially altered to chlorite.

Three layers of banded iron formation, less than 1 m thick, could be followed for a few tens of metres along strike in the lower amphibolitic greenstone unit. They are laminated at 1–5 cm scale, with irregular alternating layers of quartz and magnetite; one, however, is regularly banded with a layering of up to 10 cm. Quartz bands comprise about 50% of this rock type.

Ultramafic rocks form irregular, up to *c.* 300 m long lensoid bodies close to the base of the supracrustal succession (Figs 3, 5). The ultramafic rocks are homogeneous to slightly banded. On weathered surfaces they have a typical reddish to brown colour; on fresh surfaces they are generally black to dark grey. They consist predominantly of amphiboles, pyroxenes, chlo-

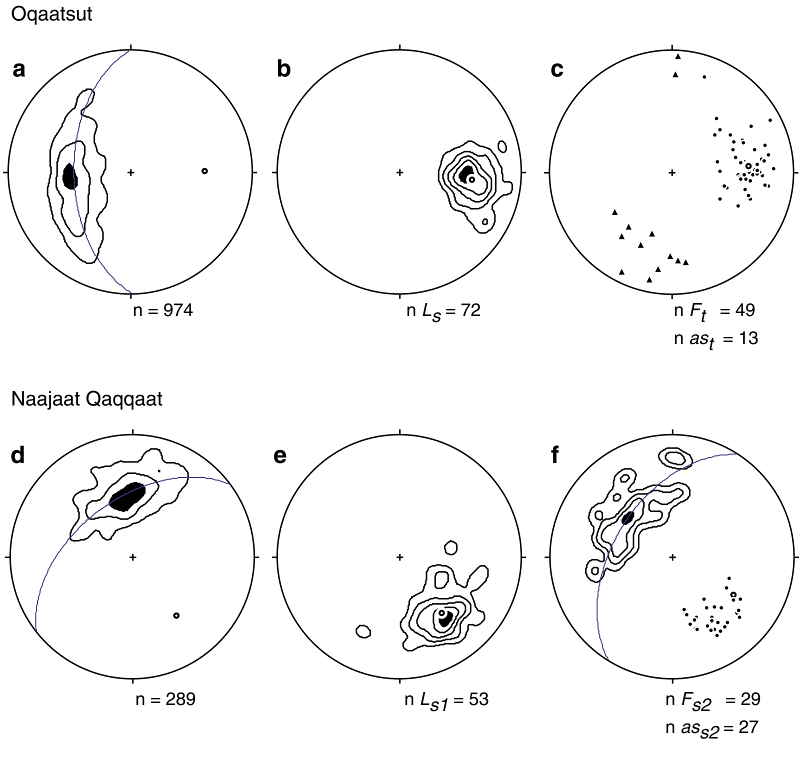

Fig. 6. Lower hemisphere equal-area projections of foliations, lineations and folds, Oqaatsut and Naajaat Qaqqaat. **a**: Poles to foliation, Oqaatsut, contoured at 1, 3 and 6%. The pole to the best fit great circle is 89/39 (open circle). **b**: $L_s$ lineations, reorientated during $D_t$, Oqaatsut, contoured at 1, 3, 6, 10 and 15%. The mean linear vector is 96/40. **c**: Attitude of $F_t$ folds, Oqaatsut. Black dots: hinge lines, triangles: poles to axial surfaces. The mean linear vector to $F_t$ hinge lines is 87/37. **d**: Poles to foliation, Naajaat Qaqqaat, contoured at 1, 3 and 6%. The pole to the best fit great circle is 142/39. **e**: $L_{s1}$ lineation, Naajaat Qaqqaat, contoured at 1, 3, 6, 10 and 15%. The mean linear vector is 143/41. **f**: Attitude of $s_2$ drag folds, Naajaat Qaqqaat. Poles to axial surfaces are contoured at 1, 3, 6 and 10%. Black dots: hinge lines to $F_{s2}$ folds. The pole to the best fit great circle to $F_{s2}$ axial surfaces is 122/40. Not shown: the mean linear vector to $F_{s2}$ hinge lines (145/40; Pedersen 1995).

rite and opaque minerals. Amphibole is mostly anthophyllite and cummingtonite, locally tremolite. Strongly metasomatised rocks consisting almost entirely of chlorite and opaque minerals also occur. Ultramafic bodies are often associated and interlayered with amphibolites and amphibole-rich schists, and in some places also with the conglomerate. The amphibolitic rocks are fine to medium grained, and appear as black layers and lenses within the ultramafic bodies.

## Structures

### *Oqaatsut*

The supracrustal sequence on Oqaatsut has a moderately steep E-dipping penetrative foliation (Fig. 6a), which is 10–20° steeper at the contact to the eastern granitoids than in the west. A similar increase in the dip of foliation is seen from south to north. Mineral lineations and crenulation lineations follow the general E-dipping structural trend (Fig. 6b).

Four stages of deformation can be distinguished in the supracrustal rocks on Oqaatsut. An early stage of isoclinal folding ($D_r$) is preserved as local remnants of isolated recumbent folds that plunge down the dip of the foliation plane. Extension of fold limbs caused boudinage of foliation-parallel competent layers (Fig. 7).

Moderately E-dipping as well as moderately to steeply N-dipping shear zones ($D_s$) occur at the contact between the eastern granitoids and the upper amphibolitic greenstone unit. Mineral lineations and shear sense indicators (rotated plagioclase crystals) show that the hanging wall has moved towards the NW. Two poorly exposed, moderately E-dipping shear zones have been recognised in the upper amphibolitic greenstone unit just above and at the contact to the middle sedimentary unit. In the southern part of the western granitoid complex imbricated quartz boudins in a moderately N-dipping $D_s$ shear zone also indicate movement of the hanging wall towards the NW (Pedersen 1995).

Upright to steeply inclined concentric folds, developed during later penetrative deformation ($D_t$, Fig. 6c), are prominent within the supracrustal rocks. They have a wavelength of the order of 10–20 m. The fold axis ($F_t$), constructed from poles to foliation planes, plunges 40°E (Fig. 6a). The contact between the supracrustals and the granitoid rocks was folded into cuspate-lobate folds due to competence contrasts, the granitoids being the most competent. This phase of folding has also affected the E- and NE-dipping $D_s$ shear zones. $D_t$ deformation has also resulted in folding of the boudins mentioned above (see Fig. 7).

The last phase of deformation observed ($D_u$) is expressed as dextral horizontal displacements along steep NW-striking brittle faults (Fig. 1), which also cut the dolerite and lamprophyre dykes. Displacements were less than 100 m.

Fig. 7. Boudinaged and folded amphibolitic band in the metasediments at the southern coast of Oqaatsut.

## *Naajaat Qaqqaat*

On Naajaat Qaqqaat the foliation dips and the mineral lineation plunges SE (Fig. 6d, e). The dip of the foliation increases from *c.* 30° at the gneiss contact to *c.* 80° near Torssukatak.

Only three of the four deformation phases on Oqaatsut have been recognised in the supracrustal rocks at Naajaat Qaqqaat ($D_r$, $D_s$ and $D_u$). $D_s$ has here been subdivided into $D_{s1}$, $D_{s2}$ and $D_{s3}$ in order to separate structures which appear to be genetically related (Pedersen 1995).

The oldest structures ($D_r$) are local recumbent isoclinal folds. They plunge S–SE with gently SE-dipping axial surfaces. During subsequent deformation ($D_{s1}$) a moderately SE-plunging penetrative *L-S* fabric was accompanied by formation of SE-dipping shear zones (Figs 5, 6e-d). Rotated garnet and staurolite crystals suggest movement of the hanging wall towards NE. Close asymmetric *Z* drag folds ($F_{s2}$) with SE-dipping axial surfaces and moderately S–SE plunging axes represent a late stage of the NE-directed shear movements (Figs 4, 6f). Drag folds ($F_{s2}$) developed at a high angle to the transport direction as a result of a minor unconformity between the lithologies and the shear plane. In response to progressive strain both axial surfaces and fold axes were re-oriented. Axial surfaces were rotated towards the shear plane and the $F_{s2}$ fold axes were rotated within their axial planes into the transport direction as illustrated by the subparallel orientation of $F_{s2}$ fold axes and the $L_{s1}$ lineations (Fig. 6e–f). Overprinting of $D_{s2}$ drag folds on the isoclinal $F_r$ folds produced local hook-interference patterns (Thiessen & Havland 1986).

$F_r$ and $F_{s2}$ folds were weakly overprinted by gently SE-plunging $F_{s3}$ folds, with upright axial surfaces and a wavelength of *c.* 100 metres. The general increase in dip of the foliation from the gneissic contact towards Torsukattak and an apparent repetition of some of the lithologies indicate imbricated piggyback thrust stacking (Pedersen 1995).

The area was cut by late, steep N–S and NW–SE striking conjugated brittle faults ($D_u$). Less than 250 m of horizontal sinistral displacement was recorded from the N–S faults; the NW–SE faults had dextral strike slips not exceeding 100 m.

## *Structural correlation between Oqaatsut and Naajaat Qaqqaat*

Naajaat Qaqqaat and Oqaatsut have a common structural chronology: an early stage of folding being followed by ductile shearing and a late stage of brittle faulting. In spite of this, a straightforward structural correlation across Torsukattak cannot be established

Table 1. Major element compositions of quartz-biotite schists from Oqaatsut and Naajaat Qaqqaat

| GGU no | 354479<br>Oq | 354320<br>Oq | 354335<br>Oq | 354397<br>NQ | 348928<br>NQ | 349122<br>NQ | 349190<br>NQ | 349196<br>NQ |
|---|---|---|---|---|---|---|---|---|
| $SiO_2$ | 66.88 | 67.04 | 68.54 | 68.30 | 65.95 | 67.07 | 66.42 | 64.93 |
| $TiO_2$ | 0.39 | 0.46 | 0.45 | 0.43 | 0.49 | 0.55 | 0.56 | 0.59 |
| $Al_2O_3$ | 15.82 | 16.35 | 15.60 | 15.20 | 16.41 | 16.08 | 15.21 | 15.65 |
| $Fe_2O_3$ | 0.70 | 0.72 | 0.28 | 1.12 | 0.47 | 1.02 | 1.07 | 1.80 |
| FeO | 3.57 | 2.99 | 3.21 | 3.63 | 3.85 | 3.82 | 3.37 | 4.11 |
| MnO | 0.07 | 0.05 | 0.04 | 0.07 | 0.06 | 0.08 | 0.07 | 0.12 |
| MgO | 2.53 | 1.66 | 2.59 | 1.38 | 2.03 | 1.92 | 2.34 | 3.06 |
| CaO | 2.28 | 4.19 | 3.55 | 3.09 | 1.83 | 2.48 | 3.98 | 3.67 |
| $Na_2O$ | 3.79 | 3.75 | 3.41 | 3.71 | 4.89 | 3.15 | 3.70 | 2.81 |
| $K_2O$ | 2.37 | 1.65 | 0.69 | 1.77 | 2.41 | 2.18 | 1.74 | 1.98 |
| $P_2O_5$ | 0.11 | 0.11 | 0.10 | 0.11 | 0.17 | 0.17 | 0.14 | 0.14 |
| LOI | 0.87 | 0.49 | 1.10 | 0.51 | 0.51 | 0.69 | 0.81 | 0.49 |
| Total | 99.36 | 99.46 | 99.55 | 99.32 | 99.07 | 99.21 | 99.40 | 99.34 |

Oq: Oqaatsut; samples are from the middle metasedimentary unit.

NQ: Naajaat Qaqqaat; all samples from the lower quartz-biotite schist unit.

Major elements (wt%) analysed by XRF on glass discs at the Geological Survey of Denmark and Greenland. $Na_2O$ by AAS.

LOI: loss on ignition (1000°C).

because of marked differences in structural style and orientation (Pedersen 1995). The structures at Oqaatsut dip moderately E whereas at Naajaat Qaqqaat SE dips prevail (Fig. 6). At Naajaat Qaqqaat $D_{s2}$ axial surfaces are closely related to SE-dipping shear planes, whereas on Oqaatsut $D_t$ axial surfaces cut thrusts at a high angle, which led to folding of the $D_s$ shear plane.

## Geochemistry

When dealing with the chemistry of metamorphic rocks it is important to consider the issue of secondary mobilisation of elements, and care must be exercised with respect to interpretations based on geochemical data. Alteration and metamorphism most commonly affect concentrations of the following oxides and elements: $SiO_2$, $Al_2O_3$, CaO, MgO, $K_2O$, $Na_2O$, $H_2O$, $CO_2$, Rb, Sr, Ba, Th, U and the $Fe^3/Fe^2$ ratio, whereas $TiO_2$, $P_2O_5$, total Fe, Ni, Cr, V, Zr, Y, Nb, Ce, Ga, Sc and REE (Rare Earth Elements) tend to be less affected, and therefore more useful to evaluate original geochemical characteristics (Winchester & Floyd 1977; Condie 1981; Wilson 1989).

Low loss on ignition for the analysed samples (LOI generally < 2.0 for amphibolites and < 1.0 for metasediments; Tables 1, 2) suggests that secondary hydrothermal alteration may not have been very significant since these values correspond to the range of loss on ignition for fresh unaltered basic volcanic rocks (0.5–2.0%).

### *Metasediments*

Major element analyses of metasedimentary schists from Oqaatsut and Naajaat Qaqqaat (Table 1) show that they probably were derived from (pelitic) greywackes (Rasmussen 1992). In geochemical discrimination diagrams (Fig. 8; Bathia 1983) the rocks plot in or close to the field of 'continental island arc' sediments (which includes greywackes deposited in a deep-sea environment within a back-arc region). Such a tectonic setting would be in agreement with the occurrence of the sediments in a mixed sequence with basic volcanic rocks.

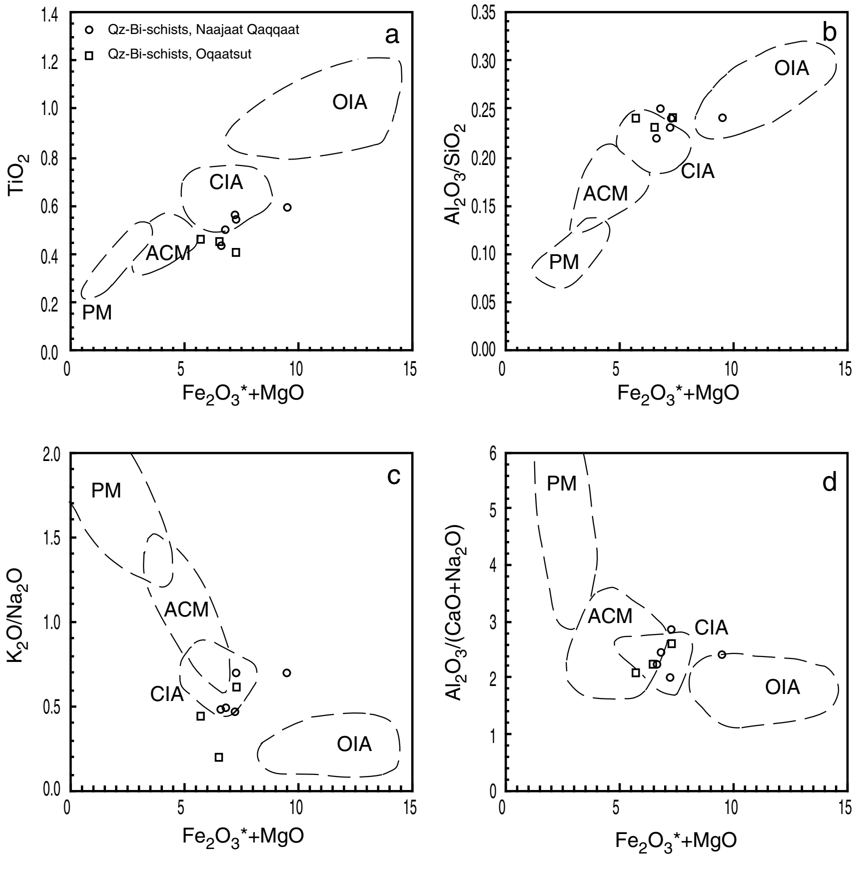

Fig. 8. Major element composition plots of quartz-biotite schists for tectonic setting discrimination (Bhatia 1983). $TiO_2$, $Al_2O_3/SiO_2$, $K_2O/Na_2O$ and $Al_2O_3$/(CaO+$Na_2O$) versus ($Fe_2O_3^{tot}$ + MgO). Data from Table 1 recalculated to 100% volatile free. Dashed lines mark the major fields of rocks representing various tectonic settings. OIA: oceanic island arc; CIA: continental island arc; ACM: active continental margin; PM: passive margin.

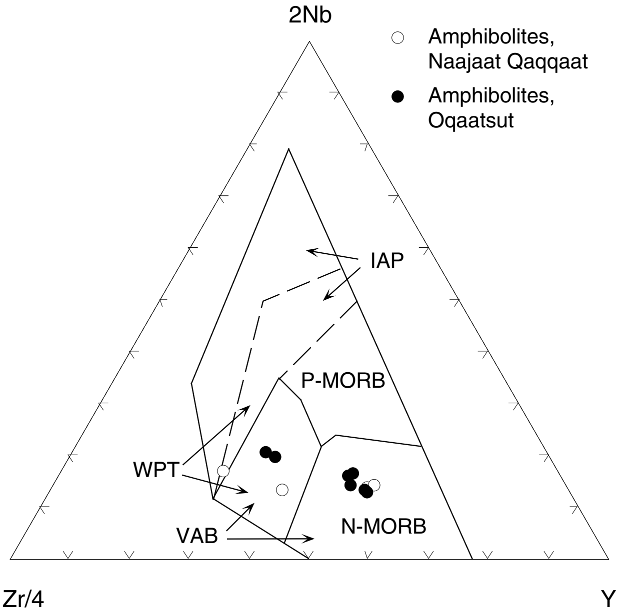

Fig. 9. Nb-Zr-Y discrimination diagram for tectonic setting for basaltic volcanic rocks (Meschede 1986). IAP: within-plate alkali basalts; WPT: within-plate tholeiites; VAB: volcanic arc basalts; P-MORB: plume-type MORB; N-MORB: normal MORB. The majority of samples from the two study areas fall in the N-MORB field, whereas four samples fall close to or within the volcanic arc basalt field.

## *Amphibolites*

Representative major and trace element analyses of amphibolites and metagabbroic rocks from both study areas (Table 2) show that the rocks have compositions typical of Mg- and Fe-rich tholeiites. Discrimination between within-plate, volcanic arc, and N- and P-type MORB basalts can in some cases be accomplished in a Nb-Zr-Y diagram (Meschede 1986). In this diagram most samples plot in the N-MORB field, but four of the samples plot close to or within the volcanic arc basalt field (Fig. 9). In a MORB-normalised multi-element diagram (Fig. 10) the four samples which plot in the volcanic arc field in the Nb-Zr-Y diagram (Fig. 9) show strong LILE (Large Ion Lithophile Elements) enrichment and a distinct positive Ce anomaly (Fig. 10a); this is not seen for the rest of the samples, which show rather flat MORB-normalised patterns (Fig. 10b). It is interesting that some samples show these MORB characteristics, since Archaean ocean floor basalts with geochemical signatures similar to modern N-MORB are very scarce or rarely preserved in the Archaean geological record (Condie 1990, 1994).

The four samples that show strong enrichment in LILE are also characterised by high Th (1–11 ppm), compared to the low LILE (MORB-like) samples which

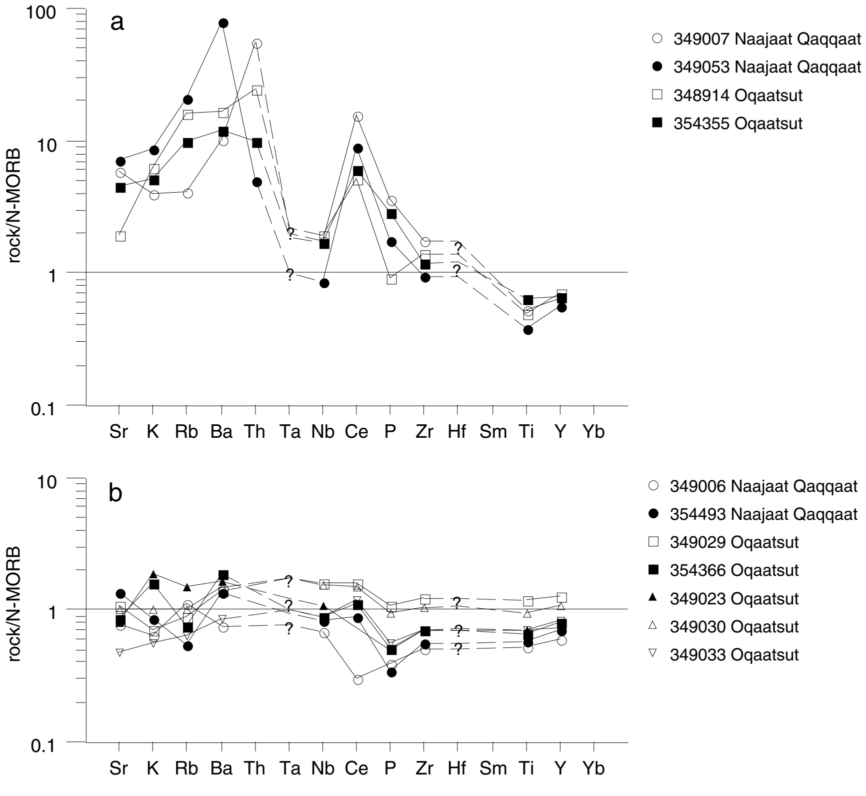

Fig. 10. N-MORB normalised variation diagrams (Pearce 1983) for selected amphibolites from Oqaatsut and Naajaat Qaqqaat. Levels of Ta and Hf (not analysed) are based on their accepted ratios in basaltic rocks with Nb and Zr, respectively (e.g. Jochum *et al.* 1986; Condie 1994). **a**: Samples of amphibolites showing strong LILE enrichment coupled with a strong positive Ce anomaly relative to Nb. **b**: Basic amphibolites showing a flat N-MORB normalised pattern suggesting an oceanic origin.

Table 2. Major and trace element compositions of amphibolites from Naajaat Qaqqaat and Oqaatsut

| GGU no | 349006 | 349007 | 349053 | 354493 | 348914 | 349023 | 349029 | 349030 | 349033 | 354355 | 354366 |
|---|---|---|---|---|---|---|---|---|---|---|---|
| | NQ | NQ | NQ | NQ | Oq | Oq | Oq | Oq | Oq | Oq | Oq |
| $SiO_2$ | 48.51 | 53.80 | 42.43 | 46.99 | 55.33 | 48.24 | 50.45 | 49.72 | 48.00 | 54.26 | 50.49 |
| $TiO_2$ | 0.78 | 0.78 | 0.56 | 0.86 | 0.74 | 1.04 | 1.76 | 1.40 | 1.01 | 0.96 | 0.98 |
| $Al_2O_3$ | 14.95 | 14.60 | 18.05 | 15.19 | 15.03 | 15.48 | 13.49 | 15.73 | 14.43 | 17.57 | 14.47 |
| $Fe_2O_3$ | 1.37 | 3.01 | 2.39 | 1.76 | 1.39 | 1.76 | 2.91 | 2.24 | 1.61 | 2.13 | 1.69 |
| FeO | 10.15 | 5.75 | 7.95 | 10.75 | 7.58 | 10.34 | 12.23 | 10.21 | 10.70 | 5.50 | 9.69 |
| MnO | 0.22 | 0.15 | 0.22 | 0.22 | 0.13 | 0.20 | 0.22 | 0.19 | 0.17 | 0.13 | 0.19 |
| MgO | 8.61 | 6.25 | 10.87 | 8.11 | 5.38 | 8.18 | 5.84 | 6.17 | 7.66 | 4.55 | 7.17 |
| CaO | 10.61 | 9.84 | 10.70 | 10.95 | 8.26 | 10.43 | 9.24 | 9.74 | 8.94 | 7.84 | 10.60 |
| $Na_2O$ | 3.01 | 2.86 | 2.49 | 2.36 | 3.07 | 2.33 | 2.15 | 2.44 | 2.03 | 4.28 | 2.86 |
| $K_2O$ | 0.09 | 0.58 | 1.28 | 0.13 | 0.94 | 0.28 | 0.10 | 0.15 | 0.08 | 0.76 | 0.23 |
| $P_2O_5$ | 0.05 | 0.42 | 0.21 | 0.04 | 0.11 | 0.06 | 0.13 | 0.11 | 0.06 | 0.34 | 0.06 |
| LOI | 1.64 | 1.66 | 1.93 | 1.87 | 1.20 | 1.61 | 1.67 | 1.80 | 4.61 | 1.24 | 1.47 |
| Total | 99.99 | 99.70 | 99.08 | 99.23 | 99.16 | 99.95 | 100.19 | 99.90 | 99.30 | 99.55 | 99.90 |
| Rb | 2.2 | 8.1 | 42 | 1.1 | 32 | 3.0 | 1.8 | 2.0 | 1.3 | 20 | 1.5 |
| Ba | 15 | 204 | 1582 | 27 | 328 | 33 | 28 | 30 | 17 | 238 | 37 |
| Pb | – | 9 | 21 | – | – | 2 | 4 | 3 | – | 5 | – |
| Sr | 95 | 698 | 870 | 163 | 235 | 96 | 131 | 121 | 58 | 545 | 103 |
| La | – | 76 | 41 | – | 27 | 5 | 6 | 4 | 4 | 24 | 3 |
| Ce | 3 | 156 | 90 | 9 | 52 | – | 16 | 15 | 12 | 61 | 11 |
| Nd | 4 | 74 | 46 | 7 | 26 | 6 | 12 | 11 | 5 | 36 | 9 |
| Y | 18 | 19 | 17 | 21 | 21 | 22 | 38 | 32 | 25 | 20 | 24 |
| Th | – | 11 | 1 | – | 5 | – | – | – | – | 2 | – |
| Zr | 46 | 158 | 84 | 50 | 124 | 63 | 110 | 95 | 64 | 108 | 63 |
| Nb | 2.4 | 6.1 | 3.0 | 2.9 | 6.8 | 3.8 | 5.5 | 5.4 | 3.1 | 5.9 | 3.1 |
| Zn | 82 | 78 | 90 | 100 | 74 | 108 | 139 | 114 | 86 | 90 | 75 |
| Cu | 87 | 9 | – | 37 | 46 | 4 | 92 | 72 | 152 | 13 | 34 |
| Co | 73 | 69 | 81 | 74 | 56 | 76 | 69 | 68 | 64 | 42 | 77 |
| Ni | 158 | 263 | 222 | 159 | 89 | 131 | 56 | 94 | 103 | 68 | 70 |
| Sc | 47 | 27 | 38 | 47 | 30 | 45 | 56 | 41 | 50 | 21 | 53 |
| V | 241 | 175 | 141 | 280 | 199 | 248 | 407 | 320 | 308 | 117 | 294 |
| Cr | 343 | 437 | 488 | 334 | 27 | 605 | 114 | 161 | 337 | 91 | 170 |
| Ga | 16 | 18 | 14 | 18 | 18 | 18 | 19 | 19 | 17 | 22 | 19 |
| Zr/Y | 2.6 | 8.3 | 4.9 | 2.4 | 5.9 | 2.9 | 2.9 | 2.9 | 2.6 | 5.4 | 2.6 |
| Ti/Zr | 103.1 | 29.9 | 41.0 | 105.6 | 36.0 | 100.9 | 97.3 | 89.7 | 99.5 | 58.8 | 94.4 |
| Ce/Nb | 1.3 | 25.6 | 30.0 | 3.1 | 7.7 | | 2.9 | 2.8 | 3.9 | 10.4 | 3.6 |
| Nb/La | | 0.08 | 0.07 | | 0.25 | 0.76 | 0.92 | 1.35 | 0.78 | 0.25 | 1.03 |
| Ti/V | 19.7 | 27.0 | 24.4 | 18.9 | 22.5 | 25.6 | 26.3 | 26.6 | 20.7 | 54.3 | 20.3 |
| Zr/Nb | 19.2 | 25.9 | 28.0 | 17.2 | 18.2 | 16.6 | 20.0 | 17.6 | 20.6 | 18.3 | 20.3 |

NQ: Najaat Qaqqaat.

Oq: Oqaatsut.

Major elements in wt% analysed by XRF on glass discs at the Survey ($Na_2O$ by AAS); trace elements in ppm analysed by XRF on powder tablets at the Geological Institute, University of Copenhagen.

–: not detected.

LOI: loss on ignition (1000°C).

have Th below detection limits. The high LILE samples are also characterised by higher Ce/Nb (7.7–30.0), Zr/Y (5.4–8.3), Zr/Nb (18.3–28.0), Ti/V (22.5–54.3) and lower Nb/La (0.07–0.25), Ti/Zr (29.9–58.8) than the low LILE group, which has lower Ce/Nb (1.3–3.9), Zr/Y (2.4–3.0), Zr/Nb (17.2–20.6) and Ti/V (18.9–26.6) but higher Nb/La (0.8–1.4) and Ti/Zr (89.6–105.6). The significant difference in LILE concentrations and incompatible element ratios cannot plausibly be explained by secondary alteration and metamorphism, and must therefore be related to differences in original magma composition.

The apparent enrichment in LREE (Light REE) and Th relative to Nb for the high LILE group, relative to the low LILE samples, may reflect a subduction-zone component and may be the result either of crustal contamination or of production of magma in a mantle wedge that has been enriched in LILE and LREE during devolatilisation of a possible descending plate (Pearce 1983; Wilson 1989; Condie 1990, 1994). Condie (1990) has shown that more than 90% of the available analyses of Precambrian greenstone basalts are characterised by a subduction-zone component. Exceptions are basalts from Archaean successions where komatiites are an important component; these basalts exhibit rather flat MORB-normalised element distributions from Th to Yb (reflecting a depleted mantle source; Condie 1990) similar to the patterns seen for the present low-LILE samples. Furthermore, when plotted in an AFC-diagram (not shown; see Rasmussen 1992), the four samples showing LILE enrichment follow a trend characteristic of calc-alkaline rocks whereas the other samples follow a tholeiitic trend.

## Discussion

The range of lithologies in the Naajaat Qaqqaat and Oqaatsut supracrustal associations – ultrabasic rocks, Mg and Fe-rich tholeiites, together with minor banded iron formation and rocks of detrital sedimentary origin – is typical for Archaean greenstone belts. Geochemical data suggest that parts of the succession were laid down in an ocean floor environment. Some of the metabasic rocks have geochemical signatures similar to modern MORB whereas others, with strong enrichment in LILE and different incompatible element ratios, have an island-arc signature.

Although strong deformation to a certain extent has obscured relationships between the two chemical types, it is certain that they are closely intercalated. Modern ocean floor basalts can be formed both at mid-ocean ridges and in back-arc spreading zones. Major element compositions of basalts from these two environments are very similar; however, volcanic rocks generated in a back-arc environment generally display a more evolved trace element character, due to the influence of a descending lithosphere slab, which is not present in basalts from mid-ocean ridges (Saunders & Tarney 1984; Wilson 1989). Trace element compositions of back-arc basalts are complex, especially in altered and metamorphosed rocks, but both MORB-like and arc-like characteristics have been observed (Wilson 1989). The presence of amphibolites with complex geochemical patterns showing both MORB and arc-like characters suggests to the authors that the amphibolites from the two study areas most likely were deposited in an environment similar to a modern back-arc setting. This suggestion is in agreement with interpretations of the depositional environment of supracrustal rocks on Arveprinsen Ejland (Nielsen 1992; Marshall & Schønwandt 1999, this volume) and in the Eqi area (Stendal *et al.* 1999, this volume; M. Marker, personal communication 1996), and show that the supracrustal rocks around Torsukattak may have been laid down in more or less the same environment as those in areas further south.

The presence of the polymict conglomerate at the base of the Naajaat Qaqqaat sequence suggests that at least in the initial stages of basin formation shallow water depths were predominant. The conglomerate could be related to initial rifting of an older craton and the creation of a continental margin basin. Ultramafic rocks at the base of the sequence at Naajaat Qaqqaat could represent products of initial magmatic activity. The close proximity of Archaean basement, the polymict conglomerate and MORB-like metabasalts may be due to strong telescoping of the sequence during later deformation. The presence of major thrust zones, which have been recognised during mapping (Figs 2, 3) would be consistent with this model.

The available observations do not allow determination with certainty whether these structures are of Proterozoic or Archaean age. However, Proterozoic ductile thrusting with sense of displacent towards W and NW has been described from the area SE of Ataa (Escher *et al.* 1999, this volume), from Nuussuaq (Garde & Steenfelt 1999, this volume) and from the Uummannaq district north of Nuussuaq (Pulvertaft 1986). Shear zones in the supracrustal rocks at Oqaatsut, which post-date emplacement of the Atâ tonalite, have the same sense of displacement and could therefore also be Proterozoic. Sediments of the early Proterozoic Anap nunâ

Group on Anap Nunaa and the island to the west (Fig. 1 inset) show open to tight folds with E–W axial trends (Kalsbeek 1992; Higgins & Soper 1999, this volume), and it is plausible that $D_t$ folds on Oqaatsut with similar trends are also of Proterozoic age. Furthermore, the early Proterozoic lamprophyre dykes on Oqaatsut follow the $D_t$ structural trend, which lends support to this contention.

Garde & Steenfelt (1999, this volume) correlate the supracrustal rocks at Naajaat Qaqqaat with similar occurrences at Saqqaq and Itilliarsuup Qaqqa on the northern side of Torsukattak, and the supracrustals of Oqaatsut with those of Arveprinsen Ejland and Eqi to the south (Fig. 1 inset). Although correlation across Torsukattak is problematic for several reasons (see Garde & Steenfelt 1999, this volume) the similarities in stratigraphy, chemistry and structural style strongly suggest to the authors that the supracrustal sequences at Oqaatsut and Naajaat Qaqqaat are very closely related.

## Acknowledgements

We thank Adam Garde and Feiko Kalsbeek for critical reviews of earlier drafts of this manuscript, and our supervisors Paul Martin Holm and Lilian Skjernaa for their support during our studies.

## References

Bhatia, M.R. 1983: Plate tectonics and geochemical composition of sandstones. Journal of Geology **91**, 611–627.

Condie, K.C. 1981: Archean greenstone belts, 434 pp. Amsterdam: Elsevier.

Condie, K.C. 1990: Geochemical characteristics of Precambrian basaltic greenstones. In: Hall, R.P. & Hughes, D.J. (eds): Early Precambrian basic magmatism, 40–55. London: Blackie.

Condie, K.C. 1994: Greenstones through time. In: Condie, K.C. (ed.): Archaean crustal evolution, 85–120. Amsterdam: Elsevier.

Escher, A. & Burri, M. 1967: Stratigraphy and structural development of Precambrian rocks in the area north-east of Disko Bugt, West Greenland. Rapport Grønlands Geologiske Undersøgelse **13**, 28 pp.

Escher, J.C., Ryan, M.J. & Marker, M. 1999: Early Proterozoic thrust tectonics east of Ataa Sund, north-east Disko Bugt, West Greenland. In: Kalsbeek, F. (ed.): Precambrian geology of the Disko Bugt region, West Greenland. Geology of Greenland Survey Bulletin **181**, 171–179 (this volume).

Garde, A.A. & Steenfelt, A. 1999: Precambrian geology of Nuussuaq and the area north-east of Disko Bugt, West Greenland. In: Kalsbeek, F. (ed.): Precambrian geology of the Disko Bugt region, West Greenland. Geology of Greenland Survey Bulletin **181**, 6–40 (this volume).

Higgins, A.K. & Soper, N.J. 1999: The Precambrian supracrustal rocks of Nunataq, north-east Disko Bugt, West Greenland. In: Kalsbeek, F. (ed.): Precambrian geology of the Disko Bugt region, West Greenland. Geology of Greenland Survey Bulletin **181**, 79–86 (this volume).

Jochum, K.P., Seufert, H.M., Spettel, B. & Palme, H. 1986: The solar-system abundances of Nb, Ta and Y, and the relative abundance of refractory lithophile elements in differentiated planetary bodies. Geochimica et Cosmochimica Acta **50**, 1173–1183.

Kalsbeek, F. 1992: Large-scale albitisation of siltstones on Qeqertakavsak island, northeast Disko Bugt, West Greenland. Chemical Geology **95**, 213–233.

Kalsbeek, F. & Skjernaa, L. 1999: The Archaean Atâ intrusive complex (Atâ tonalite), north-east Disko Bugt, West Greenland. In: Kalsbeek, F. (ed.): Precambrian geology of the Disko Bugt region, West Greenland. Geology of Greenland Survey Bulletin **181**, 103–112 (this volume).

Larsen, L.M. & Rex, D.C. 1992: A review of the 2500 Ma span of alkaline-ultramafic, potassic and carbonatitic magmatism in West Greenland. Lithos **28**, 367–402.

Marshall, B. & Schønwandt, H.K. 1999: An Archaean sill complex and associated supracrustal rocks on Arveprinsen Ejland, north-east Disko Bugt, West Greenland. In: Kalsbeek, F. (ed.): Precambrian geology of the Disko Bugt region, West Greenland. Geology of Greenland Survey Bulletin **181**, 87–102 (this volume).

Meschede, M. 1986: A method of discriminating between different types of mid-ocean ridge basalts and continental tholeiites with the Nb-Zr-Y diagram. Chemical Geology **56**, 207–218.

Nielsen, A.T. 1992: Geologi, geokemi og tektonisk setting for Andersen mineraliseringen: en vulkansk massiv sulfidforekomst i det arkæiske supracrustalbælte, Arveprinsen Ejland, Vestgrønland, 98 pp. Unpublished cand. scient. thesis, Københavns Universitet, Danmark.

Pearce, J.A. 1983: Role of the sub-continental lithosphere in magma genesis at active continental margins. In: Hawkesworth, C.J. & Norry, M.J. (eds): Continental basalts and mantle xenoliths, 230–250. Nantwich, UK: Shiva Publishing Ltd.

Pedersen, L.F. 1995: Beskrivelse og analyse af deformationsstrukturer på Naajaat Qaqqaat og Oqaatsut, Disko Bugt, Vestgrønland. Indikationer på partitionering af paleostressfeltet i forbindelse med strike-slip bevægelser i Torsukattak fjorden, 158 pp. Unpublished cand. scient. thesis, Københavns Universitet, Danmark.

Pulvertaft, T.C.R. 1986: The development of thin thrust sheets and basement-cover sandwiches in the southern part of the Rinkian belt, Umanak district, West Greenland. Rapport Grønlands Geologiske Undersøgelse **128**, 75–87.

Rasmussen, H. 1992: Petrography, geochemistry and combined K/Ar and $^{40}$Ar/$^{39}$Ar mineral age investigations of Archaean amphibolitic, ultramafic and related supracrustal rocks from

Naujât qáqât and Oqaitsut, Disko Bugt, West Greenland, 149 pp. Unpublished cand. scient. thesis, University of Copenhagen, Denmark.

Rasmussen, H. & Holm, P.M. 1999: Proterozoic thermal activity in the Archaean basement of the Disko Bugt region and eastern Nuussuaq, West Greenland: evidence from K-Ar and $^{40}$Ar-$^{39}$Ar mineral age investigations. In: Kalsbeek, F. (ed.): Precambrian geology of the Disko Bugt region, West Greenland. Geology of Greenland Survey Bulletin **181**, 55–64 (this volume).

Saunders, A.D. & Tarney, J. 1984: Geochemical characteristics of basaltic volcanism within back-arc basins. In: Kokelaar, B.P. & Howells, M.F. (eds): Marginal basin geology, volcanic and associated sedimentary and tectonic processes in modern and ancient marginal basins. Geological Society Special Publication (London) **16**, 59–76.

Stendal, H., Knudsen, C., Marker, M. & Thomassen, B. 1999: Gold mineralisation at Eqi, north-east Disko Bugt, West Greenland. In: Kalsbeek, F. (ed.): Precambrian geology of the Disko Bugt region, West Greenland. Geology of Greenland Survey Bulletin **181**, 129–140 (this volume).

Thiessen, R.L. & Havland, T. 1986: A technique for analysis of refold structures. Journal of Structural Geology **8**, 191–200.

Wilson, M. 1989: Igneous petrogenesis, a global tectonic approach. 466 pp. London: Unwin Hyman.

Winchester, J.A. & Floyd, P.A. 1977: Geochemical discrimination of different magma series and their differentiation products using immobile elements. Chemical Geology **20**, 325–343.